Environmental Science and Pollution Research (2022) 29:39027–39040
https://doi.org/10.1007/s11356-021-18332-2

RESEARCH ARTICLE

Photocatalytic concrete for degrading organic dyes in water

Yiming Zhou[1,2] · Mohamed Elchalakani[2] · Houfeng Liu[3] · Bruno Briseghella[4] · Chuanzhi Sun[1]

Received: 16 July 2021 / Accepted: 21 December 2021 / Published online: 31 January 2022
© The Author(s), under exclusive licence to Springer-Verlag GmbH Germany, part of Springer Nature 2021

Abstract

Since the advent of photocatalytic degradation technology, it has brought new vitality to the environmental governance and the response to the energy crisis. Photocatalysts harvest optical energy to drive chemical reactions, which means people can use solar energy to complete some resource-consuming activities by photocatalysts, such as environmental governance. In recent years, researchers have tried to combine photocatalyst TiO_2 with building materials to purify urban air and obtained good results. One of the important functions of photocatalysts is to degrade organic pollutants in water through light energy, but this technology has not been reported in the practical application areas. To extend this technology to practical application areas, photocatalytic concrete for degrading pollutants in waters was proposed and demonstrated for the first time in this paper. The photocatalytic concrete proposed based on the K-g-C_3N_4 shows a strong ability to degrade the organic dyes. According to the experiment results, the angle of light source plays an important role in the process of photocatalytic degradation, while waters with pH value of 6.5–8.5 hardly influenced the degradation of organic dyes. When the angle of light source is advantageous for photocatalytic concrete to absorb more visible light, more organic dyes will be degraded by photocatalytic concrete. The degradation rate of methylene blue could reach about 80% in ½ hour under desirable conditions and is satisfied compared with that of reported works. This study implicates that photocatalytic concrete can effectively degrade organic dyes in water. The influences of changes in the water environment hardly affect the degradation of organic pollutants, which means photocatalytic concrete can be widely used in green infrastructures to achieve urban sewage treatment.

Keywords Photocatalyst · Photocatalytic concrete · G-C_3N_4 · Solar energy · Pollutants · Degradation

Introduction

The photocatalytic effect, as a new technology of utilizing light energy, has attracted much attention in recent years (Akpan and Hameed 2009; Mirzaei et al. 2016; Ameta et al. 2018; Ye et al. 2019; Tahir et al. 2020). The photocatalytic effect is defined as the catalytic oxidation reaction of photocatalysts under light, also known as photocatalysis (Serpone 2000). Photocatalysis can achieve many functions such as hydrogen production, air purification, degradation of dyes, and antibiotics (Baghriche et al. 2017; Abou Saoud et al. 2018; Zeghioud et al. 2019). The above-mentioned functions can be achieved only by sunlight. Therefore, photocatalysts are being brought into many different areas to achieve novel functions (Yamashita et al. 2008; Suarez et al. 2014; Li et al. 2015; Zeghioud et al. 2018, 2021; Mori et al. 2020; Zhou et al. 2021). However, such a kind of highly promising material has not been utilized widely in the field of green building materials. Most concrete structures in cities receive tremendous solar energy within their lifespan and the use of this type of energy is still somewhat limited. If photocatalysts could be applied on the surface of construction materials, a new path for using this part of solar energy will be illuminated. Therefore, a few scholars tried to add a kind of photocatalyst TiO_2 in road construction materials to achieve degradation of NOx of air and got ideal results (Beeldens 2006; Folli et al. 2012; Jiménez-Relinque et al. 2019; Yu et al. 2020a, b; Singh et al. 2021). However, few scholars in the field of green building materials pay attention

Responsible Editor: Sami Rtimi

Highlights
- Photocatalytic concrete based on K-g-C_3N_4 was developed.
- Photocatalytic concrete was used to degrade organic dyes in water.
- the deep roots of influences of environmental factors on photocatalytic concrete were discussed in detail

✉ Chuanzhi Sun
suncz@sdnu.edu.cn

Extended author information available on the last page of the article

to another potential function of photocatalysts—degradation of pollutants (Frederichi et al. 2021). According to Houas et al. (2001), Bhatkhande et al. (2002), Sakthivel et al. (2003), and Akpan and Hameed (2009), photocatalysts can degrade organic pollutants in the water. This function has the potential to be applied to the surface of materials that contact polluted water in cities. For example, photocatalytic materials can be used on the surface of city hydraulic structures to clean rivers polluted by organic dyes (as shown in Fig. 1). Therefore, we proposed photocatalytic concrete for degrading organic dyes in water in this study.

In this study, one photocatalyst graphite-like carbon nitride (g-C_3N_4) that has gained much attention in the field of chemistry was used to develop photocatalytic concrete materials. g-C_3N_4 is a kind of potential photocatalytic material and was first synthesized in 1993 (Cao and Yu 2014; Wen et al. 2017; Fu et al. 2018). g-C_3N_4 is a semiconductor material and composed of two elements widely distributed on the earth—carbon and nitrogen. The solar energy utilization efficiency of g-C_3N_4 is much higher than that of traditional photocatalytic materials such as TiO_2 reported previously. Specifically, TiO_2 can only use a small part of sunlight (ultraviolet) so TiO_2 cannot make full use of the energy of sunlight. The specific reasons are as follows: For different kinds of photocatalysts, they have different absorption threshold λ_g and can only absorb the light wavelength smaller than λ_g (Sayama et al. 1996; Li et al. 2013). Furthermore, the absorption threshold λ_g of photocatalysts is decided by their band gap E_g. The relationship between them is as follows (Yin et al. 2013):

$$\lambda_g(\mathrm{nm}) = \frac{1240}{E_g(\mathrm{eV})} \quad (1)$$

where 1240 is the product of Planck constant and the velocity of light in a vacuum. According to formula (1), it can be seen that the smaller band gap E_g is, the bigger absorption threshold λ_g is. However, the band gap of TiO_2 is wide (3.2 eV) and the absorption threshold λ_g is 387 am (Fonseca et al. 2015). Therefore, TiO_2 can only absorb ultraviolet light with a wavelength less than 387 am to produce a photocatalytic reaction, while ultraviolet light only accounts for about 5% of solar energy (Jacobson 1999; Zou et al. 2001). The light energy received by a concrete structure in its entire lifespan is mostly solar energy (sunlight), so TiO_2 photocatalyst cannot make full use of the light energy when it is used to make photocatalytic concrete materials. However, for g-C_3N_4, the band gap is only about 2.7 eV (Yang et al. 2016). It can absorb ultraviolet light with a wavelength greater than 387am and produce a photocatalytic reaction. The utilization rate of solar energy of g-C_3N_4 is more than 10 times that of TiO_2 (Liu et al. 2019a, b). In addition, TiO_2 is suspected to be oncogenic according to related chemical research (Urrutia-Ortega et al. 2016; Nasr et al. 2018), so it is not appropriate to use TiO_2 on the surface of structures that contact water bodies directly. In contrast, g-C_3N_4 is a kind of non-metallic semiconductor, which is composed of two elements widely distributed on the earth—carbon and nitrogen. Chemical studies have proved that g-C_3N_4 is completely nontoxic and chemically stable (Tang et al. 2019; He et al. 2020). Moreover, g-C_3N_4 has strong acid and alkali corrosion resistance, which makes g-C_3N_4 suitable for concrete structures susceptible to corrosion (Pourhashem et al. 2020). In addition to the advantages of g-C_3N_4 as photocatalysts above, g-C_3N_4 is easy to be modified to be more active by morphology control, semiconductor recombination, element doping, and molecular doping (Liu et al. 2019a, b). Considering the positive aspects of g-C_3N_4 above, we modified g-C_3N_4 by doping with potassium and the modification improved the ability of g-C_3N_4 to absorb visible light. Furthermore, K-Doped g-C_3N_4 was combined with the surface of concrete materials to make concrete materials capable of degrading organic dyes in water. Under visible light, the photogenerated carriers of K-g-C_3N_4 on the surface of concrete materials can combine with hydroxyl radical (·OH), superoxide radical ($\cdot O_2$-) and hydrogen peroxide (H_2O_2) to form a variety of active oxygen-containing substances, which can degrade common organic pollutants in water, such as methylene blue and some small molecule organic compounds. According to Konstantinou and Albanis (2004), the final products of the

(a) (b)

Fig. 1 **a**, **b** Rivers polluted by organic dyes

above process are mainly CO_2 and water. The degradation mechanism is shown in Fig. 2.

Next, the degradation efficiency of K-Doped g-C_3N_4 photocatalytic concrete to degrade organic dyes in water under sunlight was tested, taking methylene blue, as the degradation target. Finally, we took regression analysis to analyze the influences of the environmental factors such as angles of lighting source and pH values of waters. The influences of the environment factors on photocatalytic performances of photocatalytic concrete were addressed quantitatively according to the results of response surface methods.

Experimental procedure

Materials

Concrete materials

Portland cement (CEM I, 42,5R) and ISO Standard sands (ISO 679:2009, quartz sands) were used to make concrete materials. The content of silica of sands is more than 96% and the loss on ignition is not more than 0.40%. The mud content (including soluble salts) of sands is not more than 0.20%. Due to limited experimental conditions, the size of mold for making concrete materials is 23 mm × 23 mm × 20 mm. Considering the size of concrete model was small and the strength of photocatalytic concrete was not affected by photocatalyst on the surface, coarse aggregates were not used in the production process of making concrete cubes (Xu et al. 2020). Therefore, the study of photocatalytic materials in this paper was completed through photocatalytic mortars.

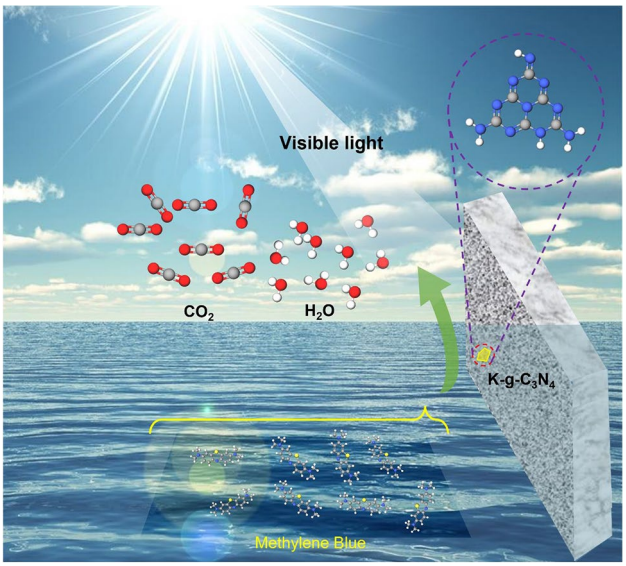

Fig. 2 Photocatalytic concrete for degrading organic dyes in water

Photocatalysts

Generally, g-C_3N_4 shows better catalytic performances after modification so we decided to use modified g-C_3N_4 as photocatalytic materials. Some scholars modified g-C_3N_4 with metal materials to improve the catalytic activity of g-C_3N_4 such as CoP/B doped g-C_3N_4, Na-g–C_3N_4 and V-g-C_3N_4 (Wang et al. 2018; Li et al. 2019). Compared with the original g-C_3N_4, the activity of g-C_3N_4 modified by metals is greatly improved, but many metals are not suitable for concrete materials. Firstly, noble metals like cobalt cannot meet the requirements of concrete materials to be low-priced construction materials. In addition, many kinds of noble metals are toxic such as vanadium. Vanadium can improve the catalytic activity of g-C_3N_4; however, vanadium will continue to pollute the environment if released out from concrete materials (Venkataraman and Sudha 2005). For low-price alkali metals like Na^+, although it is cost-effective, doping Na^+ is usually implemented through NaCl (Qing et al. 2016), which will corrode concrete and the embedded reinforcement. Thus, it is necessary to find a desirable method to modify g-C_3N_4 to improve its catalytic activity and make it suitable for concrete materials. Therefore, we used K_2SO_4 to dope K^+ to modify g-C_3N_4. Potassium is nontoxic and low-priced and the corrosion of sulfates is much lower than chlorides. Firstly, 10 g urea (purity 99%, Shanghai Macklin Biochemical Co., Ltd, Shanghai) and 0.05 g K_2SO_4 (purity 99.99%, Shanghai Aladdin Biochemical Technology Co., Ltd. Shanghai) were dissolved in 20 mL deionized water. The urea and K_2SO_4 solution is then evaporated to dryness in an oil bath at 80℃. The dried powder was put in the tube furnace at 550 °C for 3 h in air with a heating rate of 2 °C min^{-1} and the resulting products were denoted as K-g-C_3N_4 as shown in Fig. 3.

The mass ratio of sulfate in K-g-C_3N_4 prepared by the above method is only 0.5%, which is negligible according to ACI 201.2R-08. Therefore, there is a low possibility that the K-g-C_3N_4 photocatalysts will corrode the concrete materials.

Experimental model of K-g-C_3N_4 photocatalytic concrete

As for the process of combining concrete materials with photocatalysts, considering that the K-g-C_3N_4 photocatalysts should be distributed on the surface of mortars as much as possible, a direct approach was taken to attach the K-g-C_3N_4 photocatalysts to concrete surfaces as follows. According to BS EN197–1, mortar cubes of mortars were prepared as the mass ratio of cement-sand-water = 1:2:0.45. Mortar slurries were then cast into the molds (23 mm width × 23 mm

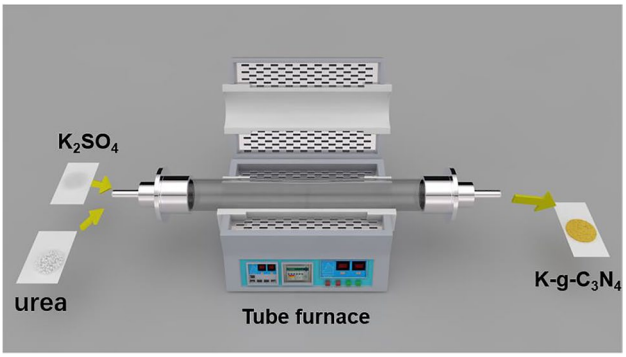

Fig. 3 K-g-C_3N_4 made by urea and K_2SO_4

length × 20 mm height) and cured at room temperature for 2 h. At this time, the hardening processes of the surface of mortars were just beginning and it was a suitable timing to let the surface of mortars combine K-g-C_3N_4 photocatalysts. At first, 0.05 g K-g-C_3N_4 was distributed on the surfaces of mortar specimens (as shown in Fig. 4(a)). Next, a glass sheet was placed on the surface of mortar specimens to cover the K-g-C_3N_4 on surfaces of mortar specimens. Finally, a 50 g weight was placed on the glass sheet. Mortars had a low degree of setting and hardening in 2 h, so K-g-C_3N_4 would be embedded in mortars under the pressure (as shown in Fig. 4(b)). Meanwhile, the glass sheet would provide uniform pressure to make the photocatalyst to be combined with concrete uniformly. Under the above conditions, mortars were set and hardened for 21 days, and finally, the glass sheet was removed and photocatalysts were exposed. The contrast between the surface of photocatalytic concrete and that of normal concrete is shown in Fig. 4(c). As can be seen from the contrast between the Fig. 4(c), pale yellow photocatalyst was spread evenly over the surface of left photocatalytic concrete compared with right normal concrete, which made concrete have the potential to degrade organic pollutants.

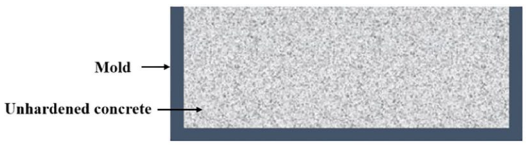

(a) Unhardened concrete

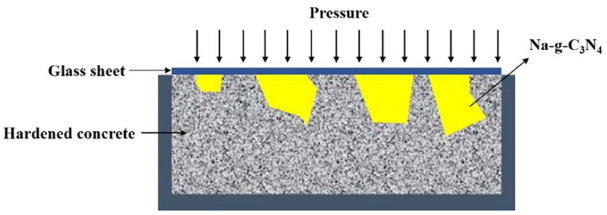

(b) Unhardened concrete

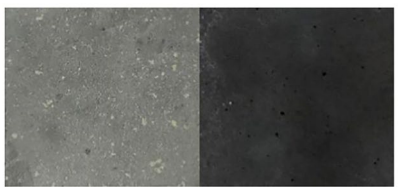

(c) Contrast between the surface of photocatalytic concrete and normal concrete

Fig. 4 Process of making photocatalytic concrete. **a** Unhardened concrete. **b** Unhardened concrete. **c** Contrast between the surface of photocatalytic concrete and normal concrete

Experiments on photocatalytic performances of degrading organic dyes

The photocatalytic performances of prepared samples (23 mm width × 23 mm length × 20 mm height) were measured in a customized quartz box (5 cm width × 5 cm length × 5 cm height) with high light transmission (Jinzhou East Quartz Material Co., Ltd., China) full of methylene blue solution (as shown in Fig. 5.). The test sample was directly placed inside the quartz box so the solutions could contact photocatalysts on the surface of the mortars. The quartz box was irradiated by a 500 W xenon lamp (Beijing China Education Au-light Co., Ltd., China) with an AM1.5 solar simulation filter (Polly et al. 2011; Yongqiang et al. 2012). Xenon lamp has black body radiation and the color temperature of xenon lamps is up to 6000 K, which is very similar to the real sun so the xenon lamp was selected to simulate the light source in this study (Miyake and Kawamura 1987). To simulate the flow of water in the natural environments, a rotating magnetic stir bar was put in the quartz box to make the solution flow.

As for photocatalytic performances of K-g-C_3N_4, in addition to the material properties of the catalyst itself, important influential factors of environments are also necessary to be considered. For the degradation of organic dyes in solutions under sunlight, the angle of light source and pH of solutions are important influential factors in the process of degradation (Zhao et al. 2013; Prasad et al. 2020). The angle of light source would greatly affect the amount of light photocatalyst receives, which directly decided the catalytic efficiency. The pH value was also necessary to be considered because the K-g-C_3N_4 has different surface charge characteristics at different pH values, and the force and affinity between organic dyes and K-g-C_3N_4 will change with the pH value (Gu et al. 2019). To research the influences of various parameters above on photocatalytic performances, the experiment was set up as follows. Firstly, the light irradiated to the concrete

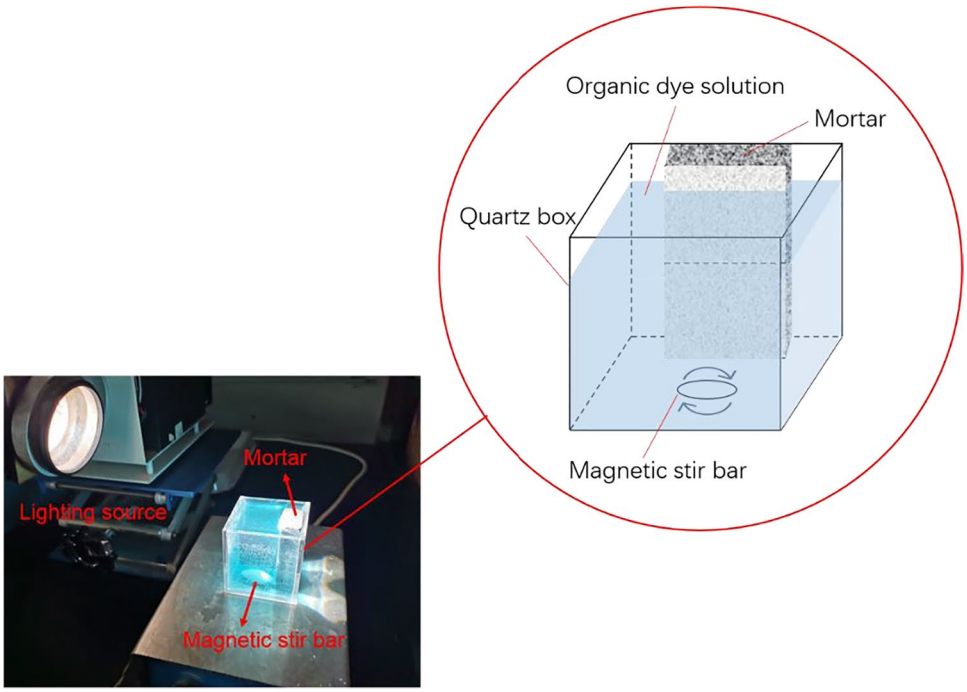

Fig. 5 The experiment on photocatalytic performances

structures in cities comes from all directions and can be divided into many types, but mainly from direct sunlight. Secondly, the angle of direct sunlight caused by latitudes and time are the main factors that affect the light intensity of an area on the earth. Therefore, we changed the irradiation angle of the xenon lamp to simulate the change of angles of sunlight. For the change of angles of sunlight caused by time, we rotated the light source around the quartz box as shown in Fig. 6(a) and this angle of light was named angle of light X_1. Furthermore, when the light source was fixed, the angle between direct light and the outer wall of the quartz box could vary with the longitudinal movement (longitudinal means the direction perpendicular to direct light) of the magnetic stirrer. Then the angles of sunlight caused by latitudes are simulated as shown in Fig. 6(b) and was named angle of light source X_2. The angle of light X_1 varied from 0° to 90° and the angle of light X_2 varied from 0° to 45°. In addition, sunlight intensity also affects photocatalytic degradation. However, the intensity of sunlight irradiated to the concrete structures is a random variable affected by many uncertain factors such as climate. Consequently, the variation of intensity of sunlight in real environments cannot be simulated. To solve the problem above, we adopted the method of shortening the experimental time. In real environments, concrete structures in cities are unlikely to be exposed to high-intensity direct sunlight for a long time due to the influences of the climate. Therefore, the change of light intensity in a day does not need to be considered as long as the photocatalytic concrete can degrade organic pollutants in a very short time under the general light intensity. Thus, we shortened the

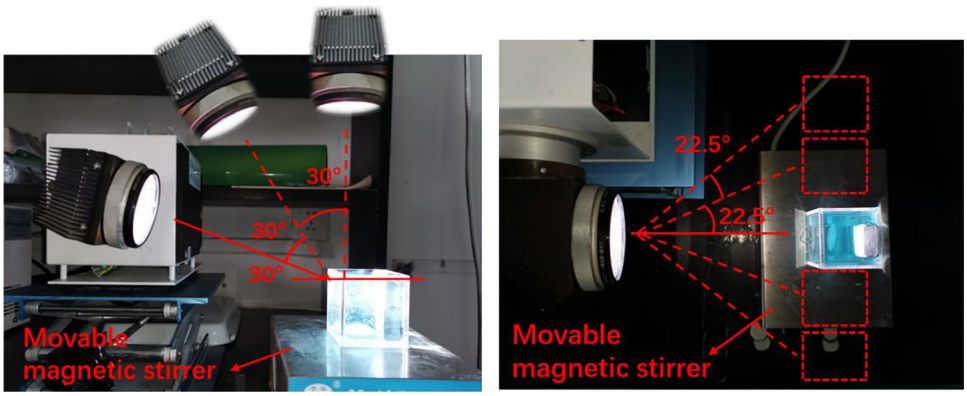

(a) Angle of light X_1 **(b)** Angle of light X_2

Fig. 6 The angles of the light source in experiments. **a** Angle of light X_1. **b** Angle of light X2

photocatalytic reaction time to 30 min, which is shorter than most degradation experiments in the field of photocatalysis.

As for concentrations of solutions, according to Ghattavi and Nezamzadeh-Ejhieh (2020) and Yu et al. (2020a, b), the concentration of organic dyes is generally from several to dozens of ppm in the photocatalytic degradation experiments by directly using g-C_3N_4 photocatalyst. Considering that the degree of photocatalytic concrete degradation of organic dyes may be lower than that of directly using catalysts, we set the concentration at 5 ppm. The concentration of methylene blue was measured by a spectrophotometer (Shanghai Metash Instruments Co., Ltd, China). The curve of absorption and concentration of methylene blue solution was obtained by the spectrophotometer (de Moraes et al. 2018). The absorbance of organic dye solutions with different concentrations (0 ppm, 1 ppm, 2 ppm, 3 ppm, 4 ppm, 5 ppm) was measured at the absorption peak ($\lambda_{max} = 665$ nm) by a spectrophotometer. Thus, we got the relationship between the concentrations of solutions and their absorbances. By obtaining the absorbance, the concentrations of solutions can also be measured by the spectrophotometer. Finally, the degradation rate of methylene blue was defined as below:

$$X(\%) = \frac{C_0 - C}{C_0} \quad (2)$$

where X is the degradation rate, and C_0 and C stand for the initial and actual concentration of methylene blue, respectively.

Results and discussions

Surface morphology and composition of K-g-C_3N_4 photocatalyst

In ideal conditions, the toxicity of productions of the photocatalytic process will be greatly reduced compared with the pollutants before degradation by g-C_3N_4 (Jiang et al. 2020). The prerequisite of conditions is that g-C_3N_4 used for the degradation has the standard microstructure of carbon nitride. If problems arise in the microstructure of g-C_3N_4 in this study, unexpected productions will be produced in the photocatalytic process. Therefore, we need to investigate the morphology and composition of K-g-C_3N_4 photocatalyst. Thus, surface morphology and composition of K-g-C_3N_4 were studied through the transmission electron microscope, scanning electron microscope, and x-ray photoelectron spectroscopy.

TEM and SEM characterizations

The morphology of prepared K-g-C_3N_4 was characterized by a transmission electron microscope (TEM, JEOL JEM-2100) and a scanning electron microscope (SEM, Hitachi SU8010), as shown in Fig. 7(a). SEM analysis indicated that the K-g-C_3N_4 prepared by high-temperature calcination method is flaky, part of which is granular and loose. The reason is that the dispersion of urea is improved during the heating process of urea, and the production of ammonia and water vapor in the reaction process is also a contributor to the formation of a loose structure. According to Fig. 7(b), the TEM micrograph showed that the K-g-C_3N_4 on concrete materials exhibits a uniform distribution structure, and the HRTEM picture of the particles reveals the clear lattice fringe of K. Note, K-g-C_3N_4 made as described above has a larger specific surface area and better photocatalytic abilities.

XPS Characterizations

The chemical compositions of prepared K-g-C_3N_4 were characterized by x-ray photoelectron spectroscopy (XPS, Escalab 250Xi). The XPS spectrum of the K-g-C_3N_4 sample is shown in Fig. 8. The XPS spectrum shows that K-g-C_3N_4 nanosheets are composed of C, N, O, and a small amount of K. The O element comes from surface adsorption or

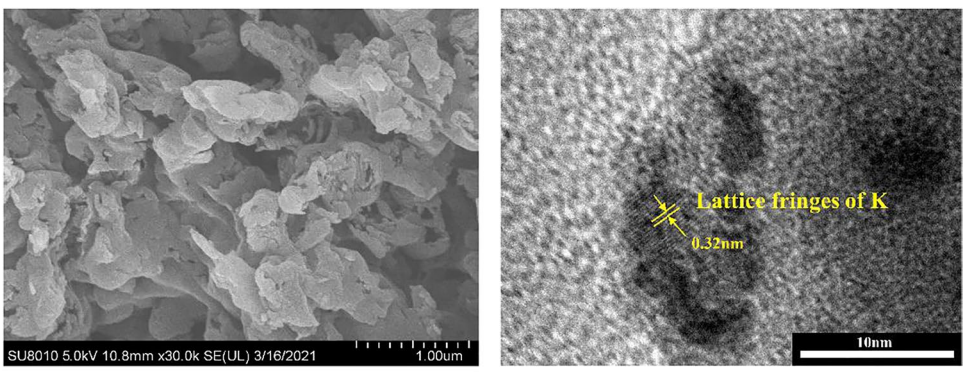

Fig. 7 Morphology of K-g-C_3N_4 on concrete materials by SEM (a) and TEM (b)

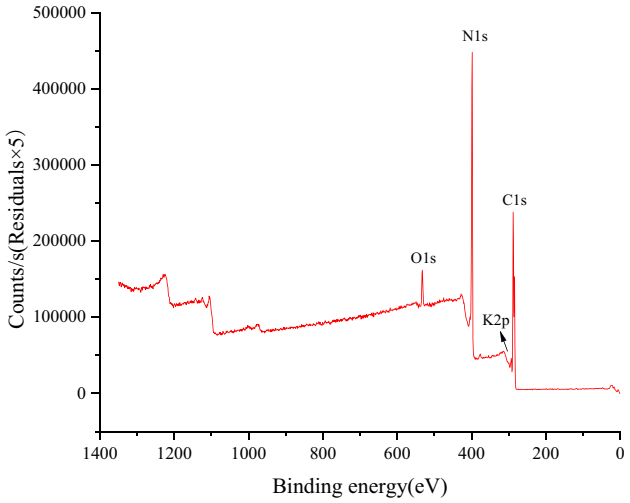

Fig. 8 XPS spectra of K-g-C_3N_4

oxidation. The elemental maps of elemental sulfur were not found in the XPS characterizations. Thus, ions were embedded in g-C_3N_4 are mainly potassium ions. Basically, sulfate ions did not enter photocatalysts. The results above illustrate the successful doping of potassium ions into the g-C_3N_4, which can boost the electrical conductivity of photocatalytic concrete under the sunlight. Then, overpotential is reduced and carrier mobilities are improved, so the photocatalytic performance is enhanced.

All the results indicate that the process for producing is successful, which means that the degradation process by prepared K-g-C_3N_4 will not bring secondary pollution.

Photocatalytic performances of K-g-C_3N_4 photocatalyst on mortars

According to Muruganandham and Swaminathan (2006) and Yu et al. (2009), 30 min was often selected as photocatalytic reaction time for degrading organic pollutants in solutions. Therefore, we used a xenon lamp to irradiate mortars for 30 min and recorded the changes of the concentration of methylene blue. Because the purpose of this chapter is to study whether the photocatalytic concrete material has the function of degrading organic dyes, we provided constant values for the angles of the light and solution pH, and set the light angle X_1 as 60°, light angle X_2 as 0°, and the solution pH as 7.5. Figure 9 shows the curve of the contrast of concentration of methylene blue under photocatalysis and without light. As can be seen that the concentration of methylene blue for the first ten minutes sightly increased. The reason is that the mortar that was just put into the solution released a small amount of powder, which leads to the decrease of light transmittance rather than the change of methylene blue concentration. The concentration of methylene blue changed immediately when the light was turned on. This indicated that a short period of illumination can trigger photocatalytic reactions of photocatalyst on concrete materials. Then, the slope of the curve showed significant changes between 20 and 30 min, which means the photocatalytic degradation rate began to be slightly accelerated in this period. After 30 min, the photocatalytic degradation rate maintained a steady rate. When the time of photocatalytic reaction reached 30 min, the degradation of methylene blue was almost 80% but the concentration of methylene blue without light hardly changed.

We compared the degradation rate of methylene blue with that of the reported works (Garcia-Segura and Brillas 2017) in the literature and the comparative table is shown as Table 1.

According to Table 1, it was apparent that photocatalytic concrete materials can decrease the concentration of methylene blue significantly compared with other photocatalysts. However, the above experiments were carried out in an ideal environment. In actual environments, the angle of sunlight changes from time to time, and waters in natural environments are complex. According to the study of Peng et al. (2019), the degradation of methylene blue will be carried out as stated below.

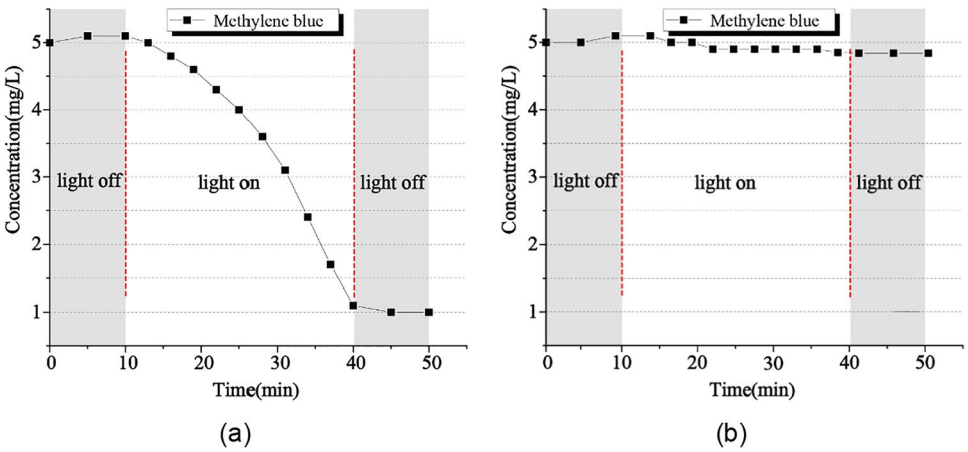

Fig. 9 The contrast of concentration of methylene blue under photocatalysis (**a**) and without photocatalysis (**b**)

Table 1 Degradation rate of methylene blue under different conditions

Dye	Initial concentration (mgL^{-1})	Experimental conditions	Degradation rate (%)
Methylene blue	5	NaCl Solution, pH 7.5, Na-g–C_3N_4 photocatalyst, 500 W Xe (> 420 nm) for 0.5 h	80%
Methylene blue	5	Na_2SO_4 Solution, pH 6.5, WO_3/$BiVO_4$ photocatalyst, 500 W Xe (> 420 nm) for 2 h	83%
Methylene blue	0.01	Na_2SO_4 Solution, $BiVO_4$ photocatalyst, visible light for 40 min	51%
Methylene blue	5	Na_2SO_4 Solution, pH 7, α-Fe_2O_3 photocatalyst, 350 W Xe for 105 min	78%
Methyl orange	5	Na_2SO_4 Solution, α-Fe_2O_3 photocatalyst, 300 W visible light for 2 h	79%
Methyl blue	10	Na_2SO_4 Solution, pH 7, $BiPO_4$ photocatalyst, 11 W UVC for 5 h	80%

Note: The first line is the experiment in this paper.

$$C_3N_4 + h\nu(> 2.7\text{eV}) \rightarrow h^+ + e^- \quad (3)$$

$$e^- + O^2 \rightarrow {}^{\bullet}O_2^- \quad (4)$$

$${}^{\bullet}O_2^- + H^+ \rightarrow H_2O_2 \quad (5)$$

$$H_2O_2 + e^- \rightarrow OH^- + {}^{\bullet}OH \quad (6)$$

$$\text{Methylene blue} + {}^{\bullet}OH \rightarrow \cdots \rightarrow CO_2 + H_2O + \cdots \quad (7)$$

We can see that the process of degradation of methylene blue is a series of chemical reactions and could be influenced by many factors, such as pH value and irradiation time (Merka et al. 2011; Rtimi et al. 2016). Therefore, it is necessary to take some influential factors into account when investigating the practical degradation abilities of photocatalytic concrete materials.

To investigate the stability of the K-g-C_3N_4 photocatalyst on the concrete material, after one photodegradation reaction, the photocatalytic concrete material was washed several times, and then the above test was repeated three times (Shao et al. 2019). The result is shown in Fig. 10. It can be seen from Fig. 10 that the degradation process of methylene blue is basically the same in the four cycle tests, which indicates that the photocatalytic process of the photocatalyst is very stable, the photocatalyst and concrete materials are firmly combined, and the catalytic activity of photocatalytic concrete material is basically unchanged in multiple cycles.

After investigating the stability of the K-g-C_3N_4 photocatalyst on the concrete material, the durability of

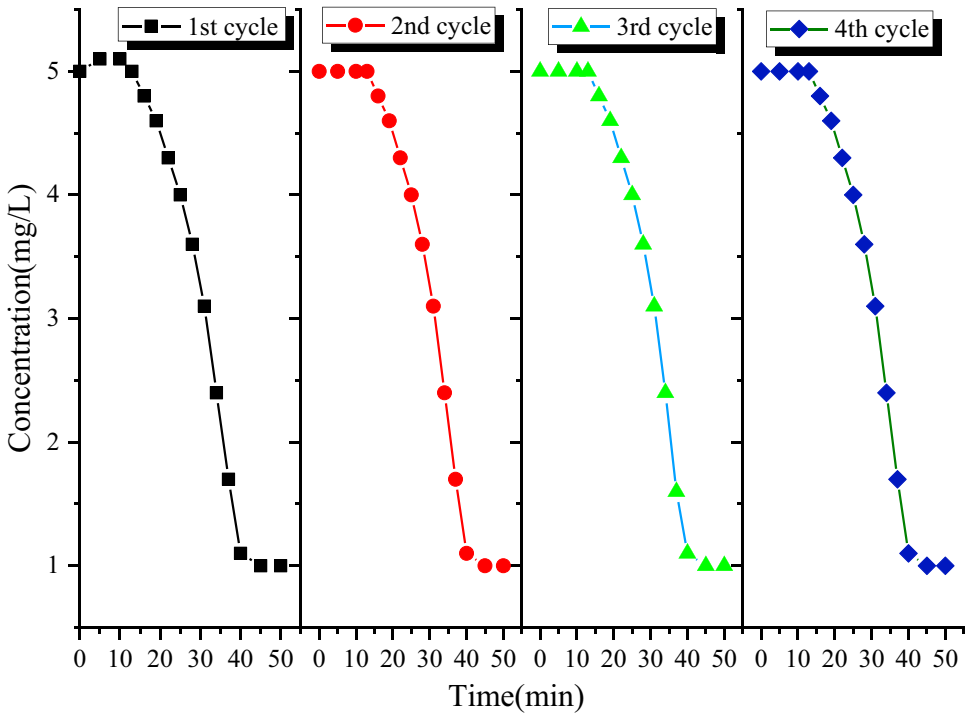

Fig. 10 The results of cycle tests

photocatalytic concrete, which will affect the service life of photocatalytic concrete, need to be discussed. The durability of photocatalytic concrete reflects in the time for that photocatalyst exists on the surface of concrete material. The photocatalytic concrete can degrade pollutants as long as the photocatalyst exists on its surface. The peeling of the surface of the concrete with time will let photocatalytic concrete lose photocatalyst. Therefore, the penetration thickness of K-g-C_3N_4 on the surface of the concrete decides the durability of photocatalytic concrete. Thus, we tested the penetration thickness of K-g-C_3N_4, we rubbed the surface of mortars with sandpaper until photocatalyst was not seen, and then we tested the change in the thickness. The change in the thickness of mortars represented the penetration thickness of photocatalyst and we found the penetration thickness of photocatalyst was about 2 mm. Next, the existing time of photocatalyst on the surface of concrete can be speculated when the speed of surface wear of concrete is obtained. In the field of civil engineering, concrete is considered isotropic material (Suidan and Schnobrich 1973; Jason et al. 2006). Consequently, each surface of mortars has the same resistance to wear and will have the same degree of wear under mass loss caused by scouring of water flow. In experiments, three surfaces of mortars contacted the water, so the following formula is obtained:

$$\frac{WL(\Delta S) + 2WH(\Delta S)}{WLH} = m \tag{8}$$

where W, L, and H represent the width, length, and height of mortars, respectively. ΔS is the thickness exfoliated of the surface of mortars under scouring of the water. M is the rate of mass loss of mortars. We can further get:

$$\Delta S + \frac{mLH}{L + 2H} \tag{9}$$

According to formula (4), ΔS can be obtained by *m, L , and H*. Thus, we measured the mass loss rate of mortars after photocatalysis experiments and used mass loss rate to calculate ΔS. The data is shown in Table 2.

Let the penetration thickness of photocatalyst is H. The length of time T that photocatalyst was able to exist on the surface of concrete can be calculated as follow:

Table 2 Rate of mass loss and ΔS of mortars

Order	Rate of mass loss/(g/6 h)	ΔS/(mm/6 h)
1	0.01%	7.3×10^{-5}
2	0.01%	7.3×10^{-5}
3	0.01%	7.3×10^{-5}
Average	0.01%	7.3×10^{-5}

$$T = \frac{H}{\Delta S} \tag{10}$$

When values of penetration thickness of photocatalyst and thickness variation are 2 mm and 7.3×10^{-5} mm/6 h, T is 1.64×10^{5} h, which means photocatalytic concrete can maintain photocatalytic performance for about 18.7 years. This is an approximate estimate for the durability of photocatalytic concrete and is valuable for the practical application.

The influences of the angle of light source and pH value of solutions

Two important factors (angle of light source and pH value of waters mentioned at the end of the "Photocatalytic performances of K-g-C3N4 photocatalyst on mortars" section) must be considered in the assessment of actual photocatalytic performances. Thus, we conducted experiments under different angles of light and pH values of waters. In each experiment, the angle of light X_1 was chosen of 0°, 30°, 60°, and 90°; the angles of light X_2 chosen were 0°, 22.5°, and 45°; the pH value was chosen of 6.5, 7.5, and 8.5. Therefore, we conducted 36 ($4\times3\times3$) different experiments. Every experiment lasted for 30 min and the degradation rate was recorded after experiments. Figure 11 shows the degradation rate of methylene blue of 36 experiments. Due to the wealth of data logged, Fig. 11 is represented in parallel coordinate plot format. In Fig. 11, four longitudinal axes are all axes of the figure. If a point is selected from each coordinate axis, and the curve formed by connecting the four points represents an experiment. Choose a data point from each coordinate axis, and then connect the four points, then forming curve represents an experiment. The four points of which the curve is composed represent the angle of light X_1, the angle of light X_2, pH value, and degradation rate of this experiment.

It can be seen from Fig. 11 that the effects of light angles and acid–base properties of solutions on the degradation of methylene blue are not intuitive and both high and low degradation rates can come from any light angles and pH value. Therefore, to study whether there is a significant relationship between the degradation rate of methylene blue and each factor, response surface methodology (RSM) was conducted (Khuri and Mukhopadhyay 2010). Response surface methodology is a method of finding the significant relationship between various reactants and end products in chemistry. Here we can regard angles of light and pH values as reactants (response factors) and the degradation result as end products (response values). Thus, the response surface methodology (RSM) can be used for analyzing the significances of influencing factors. Specifically, the response surface method of three factors can be used for experimental analysis. See Table 3 for the design of three factors.

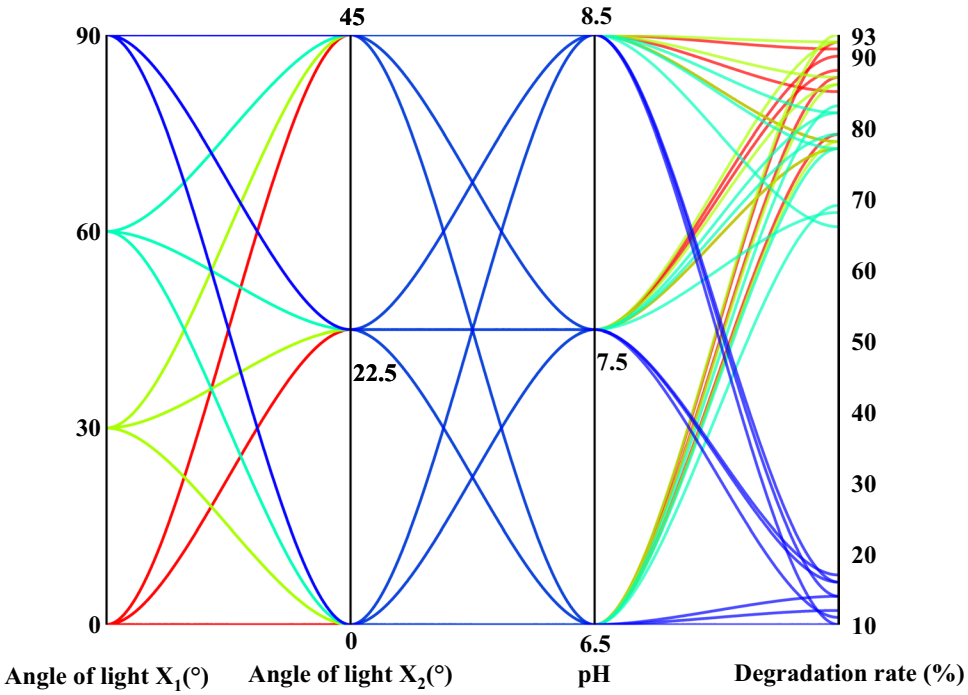

Fig. 11 degradation rate of methylene blue under the different angles of light and pH values

Table 3 Design of factors of RSM

Factors		
A (°)	B (°)	C
0	0	6.5
30	22.5	7.5
60	45	8.5
90		

Table 4 Results of several different response surface methods

Source	*P*-value	R^2	
Linear	< 0.0001	0.6272	
2FI	0.9879	0.5221	
Quadratic	< 0.0001	0.9525	Suggested

For the sake of convenience, we used A for angle of light X_1, B for angle of light X_2, and C for pH value. Then the experimental data was analyzed using Design-Expert® (Design-Expert v 7.0, Stat-Ease Inc., Minneapolis, MN). Design-Expert is the software specifically designed to conduct response surface methodology. The data for response surface methodology is that in Fig. 11 and the specific values are attached in additional file: Annex 1.

The response surface method mainly includes first-order (linear), two-factor interaction (2FI), quadratic, cubic model. To find an appropriate model for our study, *P*-value and R^2 are obtained by Design-Expert and summary of the models is shown in Table 4. According to the evaluation of several response surface methods, the quadratic model has an allowable *P*-value and the smallest value of R^2. Consequently, the quadratic model was selected in RSM analysis.

Quadratic model was fitted to the data (A, B, and C) and the regression equation was obtained as follows:

$$Y = 86.0625 - 33.7833A - 5.95833B - 0.16667C + 1.725AB + 0.5AC - 0.1875BC - 35.3125A^2 - 1.7916B^2 + 0.4167C^2 \quad (11)$$

The analysis of variance (ANOVA) was performed for formula (4) and the result is shown in Table 5.

Table 5 shows that A (angle of light X_1), B (angle of light X_2), and A^2 have a highly significant impact on the degradation rate while the other terms are insignificant. Basically, the angle of light will directly affect the light energy obtained by the catalyst on the concrete surface, thus affecting the photocatalytic degradation efficiency. The change of angle of light X_1 is similar to the change of sunlight angle in different time periods and the angle of light X_2 is similar to the change of light angle at different latitudes. However, the influences of pH value on degradation rate are not significant. Firstly, the range of pH value in the experiments is small (6.5–8.5). If the range of pH is expanded, it may change the significance of influences of pH values, but it is unnecessary to set a wide pH range considering the pH value of waters in general

Table 5 Results of analysis of variance

Source	Sum of squares	df [a]	Mean square	*F*-value	*P*-value
Model	32,616.98	9	3624.11	102.42	< 0.0001
A	22,826.2	1	22,826.27	645.10	< 0.0001
B	852.04	1	852.04	24.08	< 0.0001
C	0.6667	1	0.6667	0.0188	0.8919
AB	39.67	1	39.67	1.12	0.2994
AC	3.33	1	3.33	0.0942	0.7613
BC	0.5625	1	0.5625	0.0159	0.9006
A^2	8867.36	1	8867.36	250.60	< 0.0001
B^2	25.68	1	25.68	0.7258	0.4020
C^2	1.39	1	1.39	0.0393	0.8445

[a]df is the degree of freedom. Each term has one degree of freedom and the model has nine degrees of freedom

environments. Secondly, the influences of pH on the photocatalytic degradation of organic dyes are complex, with both advantages and disadvantages. The pH of solutions may change the electronegativity of the catalyst surface (Yamamoto and Futatsugi 2005), the aggregation in the solution, and the physicochemical properties of organic dyes. When the solution is slightly acidic, the amino group in K-g-C_3N_4 is positively charged after protonation, resulting in electrostatic repulsion with cationic dye methylene blue, which makes it difficult to be adsorbed by photocatalyst (Yamamoto and Futatsugi 2005). When the solution is alkaline, it is beneficial for the adsorption of organic dyes, but the production of · OH, which plays an important role in the photocatalytic process, is inhibited (Wang et al. 2011). In conclusion, when the pH value of solutions is in the small range around 7 (6.5–8.5), the pH value has no significant influence on the photocatalytic degradation rate of methylene blue, so the influence of pH value on degradation efficiency can be ignored.

Conclusions

In this study, the photocatalyst suitable for application to concrete materials was discussed and K-g-C_3N_4 photocatalyst was made and combined with the surface of concrete materials to prepare photocatalytic concrete. Furthermore, the photocatalytic performances of photocatalytic concrete based on K-g-C_3N_4 photocatalyst for degradation of organic dyes in water were studied. The results show that photocatalytic concrete can degrade organic dyes in water in a short time under visible light irradiation. The light angle of environmental factors has a significant impact on the degradation process of photocatalytic concrete. When enough light energy is not provided, the degradation of organic dyes in water is limited. Therefore, positioning the photocatalytic concrete relative to the sunlight must be accurately determined before construction takes place. In the case of the insufficient light source, applications of photocatalytic concrete materials and even photocatalytic concrete structures are not practical. Further research of photocatalytic concrete materials should be focused on the fields of road-building materials and shallow water hydraulic structures. However, for the pH value of water, it hardly has a significant effect on the photocatalytic reaction when it is in a small range of 6.5 to 8.5. On this limited experimental finding, one may tentatively conclude that the acid–base properties of water body in cities would have little impact on the photocatalytic reaction of photocatalytic concrete and photocatalytic concrete has potential for practical applications.

Considering the differences between the real environments and experimental conditions, such as the concentration, time under sunlight, pH value, and depth in water, the identified influences of these parameters on photocatalytic performances of photocatalytic concrete should be explained in detail:

(1) Concentration: The photocatalytic degradation can have a satisfactory result when the concentration of methylene blue is under 5 ppm.
(2) Depth of water: At present, it is observed that the degradation effect of photocatalytic concrete can be carried out approximately 5 cm below the water surface.
(3) Duration of sunlight exposure: Longer duration of sunlight exposure leads to a better degradation effect. However, photocatalytic concrete can fully perform the function of photocatalyst so it doesn't take a long time to implement a significant degradation. The degradation rate can reach about 80% under the sunlight for only 30 min.
(4) pH value: The pH value between 6.5 and 8.5 can promise the photocatalytic degradation process to proceed smoothly. Beyond this range, the photocatalytic degradation efficiency may be affected but it is unnecessary to consider an extreme pH value for normal water environments.
(5) Durability: Experimental and numerical analyses show that the durability will limit the service time of photocatalytic concrete. The specific service time of photocatalytic concrete will depend on the time of photocatalyst existing on the surface of the concrete. Currently, it could be determined that when the depth of penetration of photocatalysts is 2 mm, photocatalytic concrete can maintain its function for a relatively long period.

Supplementary Information The online version contains supplementary material available at https://doi.org/10.1007/s11356-021-18332-2.

Author contribution YZ developed the idea of the article, designed the experiments, analyzed the data, and wrote the manuscript. ME participated in writing through reviewing and editing. HL and BB contributed to the writing of the final version of the manuscript. CS revised and commented on the manuscript. All authors have read and approved the final version of the paper.

Funding This research was funded by the National Natural Science Foundation of China: 21976111; Shandong Provincial Natural Science Foundation: ZR2019MB052.

Availability of data and materials The datasets used and/or analyzed during the current study are available from the corresponding author on reasonable request.

Declarations

Ethics approval and consent to participate Not applicable.

Consent for publication Not applicable.

Competing interests The authors declare no competing interests.

References

Abou Saoud W, Assadi AA, Guiza M, Bouzaza A, Aboussaoud W, Soutrel I, Ouederni A, Wolbert D, Rtimi S (2018) Abatement of ammonia and butyraldehyde under non-thermal plasma and photocatalysis: oxidation processes for the removal of mixture pollutants at pilot scale. Chem Eng J 344:165–172. https://doi.org/10.1016/j.cej.2018.03.068

Akpan UG, Hameed BH (2009) Parameters affecting the photocatalytic degradation of dyes using TiO_2-based photocatalysts: a review. J Hazard Mater 170(2–3):520–529. https://doi.org/10.1016/j.jhazmat.2009.05.039

Ameta R, Solanki MS, Benjamin S, Ameta SC (2018) Chapter 6 – Photocatalysis. In: Ameta SC, Ameta R (eds) Advanced Oxidation Processes for Waste Water Treatment. Academic Press, New York, pp 135–175. https://doi.org/10.1016/B978-0-12-810499-6.00006-1

Baghriche O, Rtimi S, Pulgarin C, Kiwi J (2017) Polystyrene CuO/Cu_2O uniform films inducing MB-degradation under sunlight. Catal Today 284:77–83. https://doi.org/10.1016/j.cattod.2016.10.018

Beeldens A (2006) An environmental friendly solution for air purification and self-cleaning effect: the application of TiO_2 as photocatalyst in concrete. In: Proceedings of Transport Research Arena, Göteborg, Belgian Road Research Centre, Sweden

Bhatkhande DS, Pangarkar VG, Beenackers AACM (2002) Photocatalytic degradation for environmental applications–a review. J Chem Technol Biotechnol 77(1):102–116. https://doi.org/10.1002/jctb.532

Cao S, Yu J (2014) g-C3N4-based photocatalysts for hydrogen generation. J Phys Chem Lett 5(12):2101–2107. https://doi.org/10.1021/jz500546b

de Moraes NP, Silva FN, da Silva MLCP, Campos TMB, Thim GP, Rodrigues LA (2018) Methylene blue photodegradation employing hexagonal prism-shaped niobium oxide as heterogeneous catalyst: effect of catalyst dosage, dye concentration, and radiation source. Mater Chem Phys 214:95–106. https://doi.org/10.1016/j.matchemphys.2018.04.063

Folli A, Pade C, Hansen TB, De Marco T, Macphee DE (2012) TiO2 photocatalysis in cementitious systems: insights into self-cleaning and depollution chemistry. Cem Concr Res 42(3):539–548. https://doi.org/10.1016/j.cemconres.2011.12.001

Fonseca C, Ochoa A, Ulloa MT, Alvarez E, Canales D, Zapata PA (2015) Poly (lactic acid)/TiO2 nanocomposites as alternative biocidal and antifungal materials. Mater Sci Eng C 57:314–320. https://doi.org/10.1016/j.msec.2015.07.069

Frederichi D, Scaliante MHNO, Bergamasco R (2021) Structured photocatalytic systems: photocatalytic coatings on low-cost structures for treatment of water contaminated with micropollutants—a short review. Environ Sci Pollut Res 28(19):23610–23633. https://doi.org/10.1007/s11356-020-10022-9

Fu J, Yu J, Jiang C, Cheng B (2018) g-C3N4-Based heterostructured photocatalysts. Adv Energy Mater 8(3):1701503. https://doi.org/10.1002/aenm.201701503

Garcia-Segura S, Brillas E (2017) Applied photoelectrocatalysis on the degradation of organic pollutants in wastewaters. J Photochem Photobiol C 31:1–35. https://doi.org/10.1016/j.jphotochemrev.2017.01.005

Ghattavi S, Nezamzadeh-Ejhieh A (2020) GC-MASS detection of methyl orange degradation intermediates by AgBr/g-C3N4: experimental design, bandgap study, and characterization of the catalyst. Int J Hydrogen Energy 45(46):24636–24656. https://doi.org/10.1016/j.ijhydene.2020.06.207

Gu T, Dong H, Lu T, Han L, Zhan Y (2019) Fluoride ion accelerating degradation of organic pollutants by Cu (II)-catalyzed Fenton-like reaction at wide pH range. J Hazard Mater 377:365–370. https://doi.org/10.1016/j.jhazmat.2019.05.073

He F, Wang Z, Li Y, Peng S, Liu B (2020) The nonmetal modulation of composition and morphology of g-C3N4-based photocatalysts. Appl Catal B 269:118828. https://doi.org/10.1016/j.apcatb.2020.118828

Houas A, Lachheb H, Ksibi M, Elaloui E, Guillard C, Herrmann J-M (2001) Photocatalytic degradation pathway of methylene blue in water. Appl Catal B 31(2):145–157. https://doi.org/10.1016/S0926-3373(00)00276-9

Jacobson MZ (1999) Isolating nitrated and aromatic aerosols and nitrated aromatic gases as sources of ultraviolet light absorption. J Geophys Res Atmos 104(D3):3527–3542. https://doi.org/10.1029/1998JD100054

Jason L, Huerta A, Pijaudier-Cabot G, Ghavamian S (2006) An elastic plastic damage formulation for concrete: application to elementary tests and comparison with an isotropic damage model. Comput Methods Appl Mech Eng 195(52):7077–7092. https://doi.org/10.1016/j.cma.2005.04.017

Jiang J, Wang X, Zhang C, Li T, Lin Y, Xie T, Dong S (2020) Porous 0D/3D $NiCo_2O_4$/g-C_3N_4 accelerate emerging pollutant degradation in PMS/vis system: degradation mechanism, pathway and toxicity assessment. Chem Eng J 397:125356. https://doi.org/10.1016/j.cej.2020.125356

Jiménez-Relinque E, Hingorani R, Rubiano F, Grande M, Castillo Á, Castellote M (2019) In situ evaluation of the NOx removal efficiency of photocatalytic pavements: statistical analysis of the relevance of exposure time and environmental variables. Environ Sci Pollut Res 26(36):36088–36095. https://doi.org/10.1007/s11356-019-04322-y

Khuri AI, Mukhopadhyay S (2010) Response surface methodology. Wiley Interdiscip Rev Comput Stat 2(2):128–149. https://doi.org/10.1002/wics.73

Konstantinou IK, Albanis TA (2004) TiO2-assisted photocatalytic degradation of azo dyes in aqueous solution: kinetic and mechanistic investigations: a review. Appl Catal B 49(1):1–14. https://doi.org/10.1016/j.apcatb.2003.11.010

Li J, Liu Y, Zhu Z, Zhang G, Zou T, Zou Z, Zhang S, Zeng D, Xie C (2013) A full-sunlight-driven photocatalyst with super

long-persistent energy storage ability. Sci Rep 3(1):1–6. https://doi.org/10.1038/srep02409
Li H, Zhou Y, Tu W, Ye J, Zou Z (2015) State-of-the-art progress in diverse heterostructured photocatalysts toward promoting photocatalytic performance. Adv Funct Mater 25(7):998–1013. https://doi.org/10.1002/adfm.201401636
Li H, Zhao J, Geng Y, Li Z, Li Y, Wang J (2019) Construction of CoP/B doped g-C_3N_4 nanodots/g-C3N4 nanosheets ternary catalysts for enhanced photocatalytic hydrogen production performance. Appl Surf Sci 496:143738. https://doi.org/10.1016/j.apsusc.2019.143738
Liu G, Yan S, Shi L, Yao L (2019a) The improvement of photocatalysis H2 evolution over g-C3N4 with Na and cyano-group co-modification. Front Chem 7:639. https://doi.org/10.3389/fchem.2019.00639
Liu Y, Ma L, Shen C, Wang X, Zhou X, Zhao Z, Xu A (2019b) Highly enhanced visible-light photocatalytic hydrogen evolution on g-C3N4 decorated with vopc through π-π interaction. Chin J Catal 40(2):168–176. https://doi.org/10.1016/S1872-2067(18)63191-2
Merka O, Yarovyi V, Bahnemann DW, Wark M (2011) pH-control of the photocatalytic degradation mechanism of rhodamine B over $Pb_3Nb_4O_{13}$. J Phys Chem C 115(16):8014–8023. https://doi.org/10.1021/jp108637r
Mirzaei A, Chen Z, Haghighat F, Yerushalmi L (2016) Removal of pharmaceuticals and endocrine disrupting compounds from water by zinc oxide-based photocatalytic degradation: a review. Sustain Cities Soc 27:407–418. https://doi.org/10.1016/j.scs.2016.08.004
Miyake J, Kawamura S (1987) Efficiency of light energy conversion to hydrogen by the photosynthetic bacterium Rhodobacter sphaeroides. Int J Hydrogen Energy 12(3):147–149. https://doi.org/10.1016/0360-3199(87)90146-7
Mori K, Qian X, Kuwahara Y, Horiuchi Y, Kamegawa T, Zhao Y, Louis C, Yamashita H (2020) Design of advanced functional materials using nanoporous single-site photocatalysts. Chem Rec 20(7):660–671. https://doi.org/10.1002/tcr.201900085
Muruganandham M, Swaminathan M (2006) Photocatalytic decolourisation and degradation of Reactive Orange 4 by TiO2-UV process. Dyes Pigm 68(2–3):133–142. https://doi.org/10.1016/j.dyepig.2005.01.004
Nasr R, Hasanzadeh H, Khaleghian A, Moshtaghian A, Emadi A, Moshfegh S (2018) Induction of apoptosis and inhibition of invasion in gastric cancer cells by titanium dioxide nanoparticles. Oman Med J 33(2):111. https://doi.org/10.5001/omj.2018.22
Peng L, Li Z-W, Zheng R-R, Yu H, Dong X-T (2019) Preparation and characterization of mesoporous g-C3N4/SiO2 material with enhanced photocatalytic activity. J Mater Res 34(10):1785–1794. https://doi.org/10.1557/jmr.2019.113
Polly SJ, Bittner ZS, Bennett MF, Raffaelle RP, Hubbard SM (2011) Development of a multi-source solar simulator for spatial uniformity and close spectral matching to AM0 and AM1. 5. 2011 37th IEEE Photovoltaic Specialists Conference, IEEE.https://doi.org/10.1109/PVSC.2011.6186290
Pourhashem S, Duan J, Guan F, Wang N, Gao Y, Hou B (2020) New effects of TiO2 nanotube/g-C3N4 hybrids on the corrosion protection performance of epoxy coatings. J Mol Liq 317:114214. https://doi.org/10.1016/j.molliq.2020.114214
Prasad C, Tang H, Liu Q, Bahadur I, Karlapudi S, Jiang Y (2020) A latest overview on photocatalytic application of g-C3N4 based nanostructured materials for hydrogen production. Int J Hydrogen Energy 45(1):337–379. https://doi.org/10.1016/j.ijhydene.2019.07.070
Qing RP, Shi JL, Xiao DD, Zhang XD, Yin YX, Zhai YB, Gu L, Guo YG (2016) Enhancing the kinetics of Li-rich cathode materials through the pinning effects of gradient surface Na+ doping. Adv Energy Mater 6(6):1501914. https://doi.org/10.1002/aenm.201501914
Rtimi S, Giannakis S, Sanjines R, Pulgarin C, Bensimon M, Kiwi J (2016) Insight on the photocatalytic bacterial inactivation by co-sputtered TiO_2–Cu in aerobic and anaerobic conditions. Appl Catal B 182:277–285. https://doi.org/10.1016/j.apcatb.2015.09.041
Sakthivel S, Neppolian B, Shankar M, Arabindoo B, Palanichamy M, Murugesan V (2003) Solar photocatalytic degradation of azo dye: comparison of photocatalytic efficiency of ZnO and TiO2. Sol Energy Mater Sol Cells 77(1):65–82. https://doi.org/10.1016/S0927-0248(02)00255-6
Sayama K, Arakawa H, Domen K (1996) Photocatalytic water splitting on nickel intercalated A4TaxNb6-xO17 (A= K, Rb). Catal Today 28(1–2):175–182. https://doi.org/10.1016/0920-5861(95)00224-3
Serpone N, Pelizzetti E (2000) Photocatalysis. In: Fundamentals and applications. Wiley, New York. https://doi.org/10.1002/047123896 1.1608152019051816.a01
Shao B, Liu X, Liu Z, Zeng G, Liang Q, Liang C, Cheng Y, Zhang W, Liu Y, Gong S (2019) A novel double Z-scheme photocatalyst Ag3PO4/Bi2S3/Bi2O3 with enhanced visible-light photocatalytic performance for antibiotic degradation. Chem Eng J 368:730–745. https://doi.org/10.1016/j.cej.2019.03.013
Singh LP, Dhaka RK, Ali D, Tyagi I, Sharma U, Banavath SN (2021) Remediation of noxious pollutants using nano-titania-based photocatalytic construction materials: a review. Environ Sci Pollut Res:1–21. https://doi.org/10.1007/s11356-021-14189-7
Suarez S, Portela R, Hernández-Alonso MD, Sánchez B (2014) Development of a versatile experimental setup for the evaluation of the photocatalytic properties of construction materials under realistic outdoor conditions. Environ Sci Pollut Res 21(19):11208–11217. https://doi.org/10.1007/s11356-014-2725-y
Suidan M, Schnobrich WC (1973) Finite element analysis of reinforced concrete. J Struct Div 99(10):2109–2122. https://doi.org/10.1061/JSDEAG.0003623
Tahir MB, Ahmad A, Iqbal T, Ijaz M, Muhammad S, Siddeeg SM (2020) Advances in photo-catalysis approach for the removal of toxic personal care product in aqueous environment. Environ Dev Sustain 22(7):6029–6052. https://doi.org/10.1007/s10668-019-00495-1
Tang C, Liu C, Han Y, Guo Q, Ouyang W, Feng H, Wang M, Xu F (2019) Nontoxic Carbon Quantum Dots/g-C3N4 for Efficient Photocatalytic Inactivation of Staphylococcus aureus under Visible Light. Adv Healthc Mater 8(10):1801534. https://doi.org/10.1002/adhm.201801534
Urrutia-Ortega IM, Garduño-Balderas LG, Delgado-Buenrostro NL, Freyre-Fonseca V, Flores-Flores JO, González-Robles A, Pedraza-Chaverri J, Hernández-Pando R, Rodríguez-Sosa M, León-Cabrera S (2016) Food-grade titanium dioxide exposure exacerbates tumor formation in colitis associated cancer model. Food Chem Toxicol 93:20–31. https://doi.org/10.1016/j.fct.2016.04.014
Venkataraman B, Sudha S (2005) Vanadium toxicity. Asian J Exp Sci 19(2):127–134
Wang W, Zhang L, An T, Li G, Yip H-Y, Wong P-K (2011) Comparative study of visible-light-driven photocatalytic mechanisms of dye decolorization and bacterial disinfection by B-Ni-codoped TiO2 microspheres: the role of different reactive species. Appl Catal B 108:108–116. https://doi.org/10.1016/j.apcatb.2011.08.015
Wang C, Hu L, Wang M, Yue B, He H (2018) Cerium promoted Vg-C3N4 as highly efficient heterogeneous catalysts for the direct benzene hydroxylation. R Soc Open Sci 5(6):180371. https://doi.org/10.1098/rsos.180371
Wen J, Xie J, Chen X, Li X (2017) A review on g-C3N4-based photocatalysts. Appl Surf Sci 391:72–123. https://doi.org/10.1016/j.apsusc.2016.07.030

Xu Y, Jin R, Hu L, Li B, Chen W, Shen J, Wu P, Fang J (2020) Studying the mix design and investigating the photocatalytic performance of pervious concrete containing TiO2-Soaked recycled aggregates. J Clean Prod 248:119281. https://doi.org/10.1016/j.jclepro.2019.119281

Yamamoto H, Futatsugi K (2005) "Designer acids": combined acid catalysis for asymmetric synthesis. Angew Chem Int Ed 44(13):1924–1942. https://doi.org/10.1002/anie.200460394

Yamashita H, Mori K, Shironita S, Horiuchi Y (2008) Applications of single-site photocatalysts to the design of unique surface functional materials. Catal Surv Asia 12(2):88–100. https://doi.org/10.1007/s10563-008-9042-8

Yang Z, Yan J, Lian J, Xu H, She X, Li H (2016) g-C3N4/TiO2 Nanocomposites for Degradation of Ciprofloxacin under Visible Light Irradiation. ChemistrySelect 1(18):5679–5685. https://doi.org/10.1002/slct.201600861

Ye G, Yu Z, Li Y, Li L, Song L, Gu L, Cao X (2019) Efficient treatment of brine wastewater through a flow-through technology integrating desalination and photocatalysis. Water Res 157:134–144. https://doi.org/10.1016/j.watres.2019.03.058

Yin C, Zhu S, Chen Z, Zhang W, Gu J, Zhang D (2013) One step fabrication of C-doped BiVO 4 with hierarchical structures for a high-performance photocatalyst under visible light irradiation. J Mater Chem A 1(29):8367–8378. https://doi.org/10.1039/C3TA11833A

Yongqiang P, Tao B, Lingxia H (2012) Study on AM1. 5 filter in solar simulator for photovoltaic module solar simulator. Infrared Laser Eng 41(9):2484–2488

Yu K, Yang S, He H, Sun C, Gu C, Ju Y (2009) Visible light-driven photocatalytic degradation of rhodamine B over NaBiO3: pathways and mechanism. J Phys Chem A 113(37):10024–10032. https://doi.org/10.1021/jp905173e

Yu C, Zeng D, Fan Q, Yang K, Zeng J, Wei L, Yi J, Ji H (2020a) The distinct role of boron doping in Sn 3 O 4 microspheres for synergistic removal of phenols and Cr (vi) in simulated wastewater. Environ Sci Nano 7(1):286–303. https://doi.org/10.1039/C9EN00899C

Yu H, Dai W, Qian G, Gong X, Zhou D, Li X, Zhou X (2020b) The NOx degradation performance of nano-TiO2 coating for asphalt pavement. Nanomaterials 10(5):897. https://doi.org/10.3390/nano10050897

Zeghioud H, Assadi AA, Khellaf N, Djelal H, Amrane A, Rtimi S (2018) Reactive species monitoring and their contribution for removal of textile effluent with photocatalysis under UV and visible lights: dynamics and mechanism. J Photochem Photobiol A 365:94–102. https://doi.org/10.1016/j.jphotochem.2018.07.031

Zeghioud H, Kamagate M, Coulibaly LS, Rtimi S, Assadi AA (2019) Photocatalytic degradation of binary and ternary mixtures of antibiotics: reactive species investigation in pilot scale. Chem Eng Res Des 144:300–309. https://doi.org/10.1016/j.cherd.2019.02.015

Zeghioud H, Khellaf N, Amrane A, Djelal H, Bouhelassa M, Assadi AA, Rtimi S (2021) Combining photocatalytic process and biological treatment for Reactive Green 12 degradation: optimization, mineralization, and phytotoxicity with seed germination. Environ Sci Pollut Res 28(10):12490–12499. https://doi.org/10.1007/s11356-020-11282-1

Zhao C, Pelaez M, Duan X, Deng H, O'Shea K, Fatta-Kassinos D, Dionysiou DD (2013) Role of pH on photolytic and photocatalytic degradation of antibiotic oxytetracycline in aqueous solution under visible/solar light: kinetics and mechanism studies. Appl Catal B 134:83–92. https://doi.org/10.1016/j.apcatb.2013.01.003

Zhou Y, Elchalakani M, Du P, Sun C (2021) Cleaning up oil pollution in the ocean with photocatalytic concrete marine structures. J Clean Prod:129636. https://doi.org/10.1016/j.jclepro.2021.129636

Zou Z, Ye J, Sayama K, Arakawa H (2001) Direct splitting of water under visible light irradiation with an oxide semiconductor photocatalyst. Nature 414(6864):625–627. https://doi.org/10.1038/414625a

Publisher's note Springer Nature remains neutral with regard to jurisdictional claims in published maps and institutional affiliations.

Authors and Affiliations

Yiming Zhou[1,2] · Mohamed Elchalakani[2] · Houfeng Liu[3] · Bruno Briseghella[4] · Chuanzhi Sun[1]

[1] College of Chemistry, Chemical Engineering and Materials Science, Collaborative Innovation Center of Functionalized Probes for Chemical Imaging in Universities of Shandong, Shandong Provincial Key Laboratory of Clean Production of Fine Chemicals, Institute of Materials and Clean Energy, Shandong Normal University, Jinan 250014, People's Republic of China

[2] School of Engineering, Department of Civil, Environmental and Mining Engineering, University of Western Australia, 35 Stirling Hwy, Crawley, WA 6009, Australia

[3] College of Population, Resources and Environment, Shandong Normal University, Jinan 250014, China

[4] College of Civil Engineering, Fuzhou University, Fuzhou 350108, China